



HOKKAIDO UNIVERSITY

| | |
|------------------|---|
| Title | Effect of Impact Velocity in Erosive Wear of Austempered Ductile Iron |
| Author(s) | Shimizu, Kazumichi; Shiramine, Noboru; Fujita, Minoru et al. |
| Citation | 北海道大學工學部研究報告, 169, 13-19 |
| Issue Date | 1994-06-28 |
| Doc URL | https://hdl.handle.net/2115/42419 |
| Type | departmental bulletin paper |
| File Information | 169_13-20.pdf |



Effect of Impact Velocity in Erosive Wear of Austempered Ductile Iron

Kazumichi SHIMIZU, Noboru SHIRAMINE*,
Minoru FUJITA* and Toru NOGUCHI*

(Received December 24, 1993)

Abstract

Erosive wear tests were performed on austempered ductile iron (ADI) and mild steel (SS400) using a shot blast machine. Erosion damage was measured by the removed material volume at various impact angles between 10° and 90° and impact velocities of 100 and 145m/s. The mechanism of erosive wear, the effect of impact angles (α) and impact velocity (V), and the differences in wear features of the specimens were discussed.

After an initial stage, the eroded volume increases almost linearly with blasting time both in ADI and SS400, and the erosion rate in ADI is about 20% at 145m/s, 23% at 100m/s of SS400, showing that ADI has superior erosion resistance.

The surface hardness of eroded ADI specimens increased up to HV 700 from the initial HV 350 after 600s of blasting. The amount of retained austenite was measured to be about 40% of the matrix before the test, but it decreased to less than 5% by transforming to martensite, hardening the surface and practically eliminating the erosion rate markedly, and so reduces the effect of impact velocity.

1. Introduction

Surface damage caused by the impact of dispersed particles in gas or liquid flow is called erosive wear or erosion. Recently, this phenomenon is receiving much attention as a serious problem, particularly at pipe-bends or valves in pneumatic conveying systems. For instance in steel making plant, where the injection of coal dust and iron ore pellets into molten iron and steel is becoming a common technology, means to reduce erosion and methods to predict the life span of pipe-lines are urgently required. The erosive wear of pipe-lines caused by particles is complicated, and involves many factors as the velocity, impact angle, diameter of particles, and mechanical properties of material and the particles.

The authors have studied the erosion of materials for piping as mild steel and some cast irons and investigated the damage behaviors and mechanisms. Especially the influences of impact velocity on erosion in austempered ductile iron (ADI), which has excellent wear

Oita National College of Technology

Oita 870-01 Japan, Computer and Control Engineering

* Hokkaido University, Sapporo 060 Japan, Dept. of Mechanical Engineering II, Faculty of Engineering

characteristics, has been examined. To compare the results with ADI, mild steel (SS400) was also used, and based on the results, the behavior and mechanism of erosion of ADI were discussed.

2. Test specimens and experimental method

Two kinds of specimens were used : an austempered ductile iron (ADI) and a mild steel (SS400). The chemical compositions and mechanical properties are shown in Table 1 and the austempering treatment is in Figure 1. The microstructure of the specimens are in Figure 2. Figure 3 shows the shape and dimensions of the specimens. The specimen is a $50 \times 50 \times 10$ mm plate with ground surface. A sketch of the blast machine is shown in Figure 4, the machine injects particles with compressed air. Figure 5 shows the arrangement of blast machine and test stage. The specimen is fixed on a stage which enables the impact angle to be varied from 0° to 90° . The blasting grit has an average diameter of $660 \mu\text{m}$, and Vickers Hardness Number (HV) 420, and spherical ratio 96%. In every experiment 5 kg of grits were

Table 1 Chemical composition and mechanical properties of the tested irons

| | (mass%) | | | | | | |
|-------|---------|------|------|-------|-------|------|-------|
| | C | Si | Mn | P | S | Cu | Mg |
| SS400 | 0.12 | 0.13 | 0.46 | 0.022 | 0.028 | — | — |
| ADI | 3.66 | 2.15 | 0.35 | 0.021 | 0.030 | 0.53 | 0.049 |

| | σ_B | ϕ | HB | ρ |
|-------|------------|--------|-----|--------|
| SS400 | 445 | 19.7 | 150 | 7.83 |
| ADI | 1015 | 10.5 | 293 | 7.18 |

σ_B ; Tensile strength (MPa)
 ϕ ; Elongation (%)
 HB ; Brinell hardness
 ρ ; Density

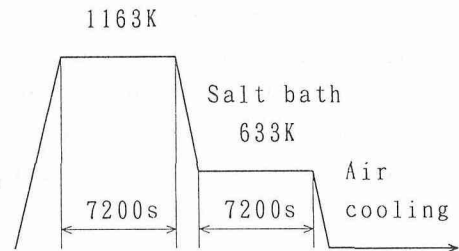


Figure 1 Austempering heat treatment

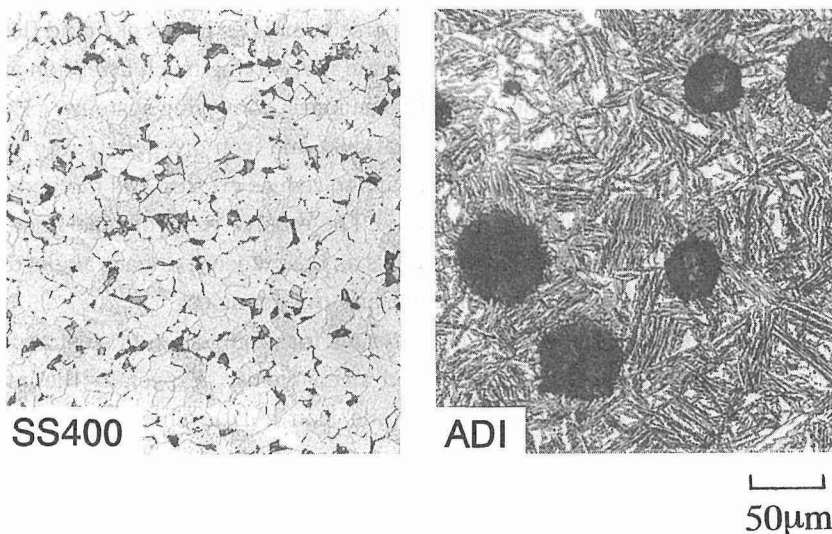


Figure 2 Microstructure of the specimens

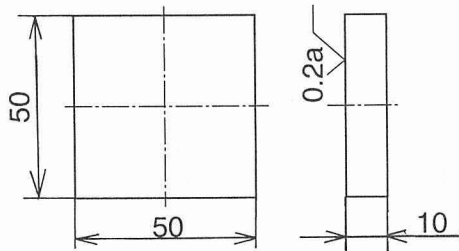


Figure 3 Test specimen

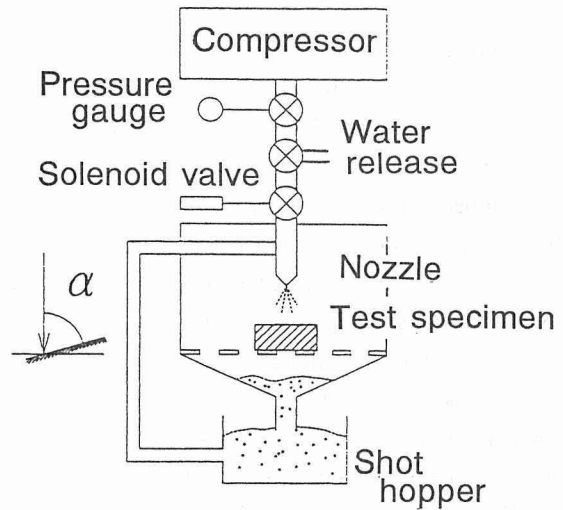


Figure 4 Outline of the shot blast machine

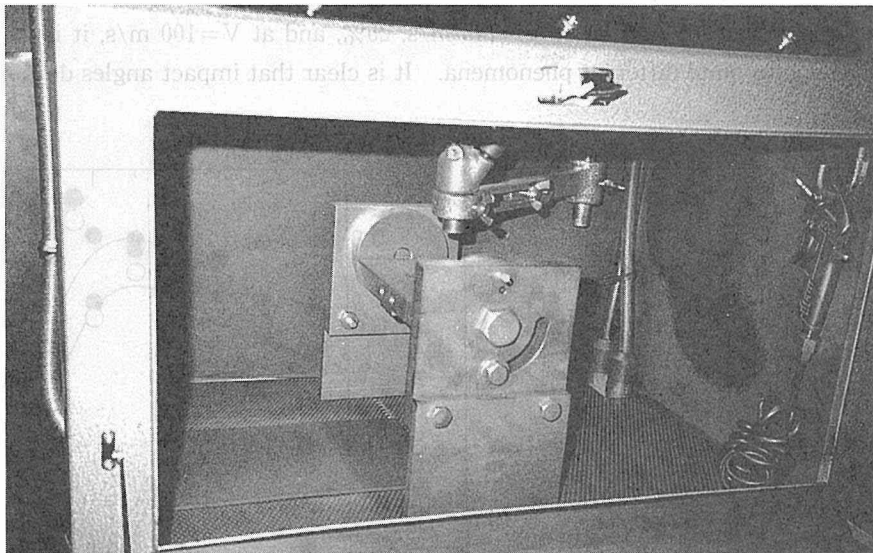


Figure 5 Nozzle and the test specimen arrangement

used and the grits were changed after every test. The tests were carried out at ambient temperatures. The impact angle was changed by 10° increments from 0° to 90° and the test time was 7200s. The eroded volume was measured by an electronic micro weight scale (0.01 mg sensitivity) after the impact experiment, and the eroded volume was determined from the mass reduction. Macroscopic and microscopic observation was performed on the eroded surface after the each test.

3. Experimental results

In discussing the erosion resistance of materials of different densities, it is not appropriate to simply compare the eroded weight of material. Therefore, by employing the average density of the materials, the eroded mass can be calculated and the erosion ratios were compared.

Figure 6 shows the relation between impact angle and erosion rate for SS400 with $V=100$ m/s and 145 m/s, blasted for 7200s. At $V=145$ m/s, the erosion rate reaches a peak at approximately 30° and at 60° reaches a minimum, after which it again starts to increase to reach a second peak at $80^\circ\sim 90^\circ$.

At $V=100$ m/s, the erosion rate reaches the maximum at about 30° , and as the impact angle increases further, the erosion rate decreases. This behavior shows an approximate correspondence to the phenomena reported for ductile materials, where the erosion rate characteristically increases with the impact angle of the particles increases. Thus, the profile of erosion characteristic in SS400 is different in impact velocity.

Figure 7 shows the relation between the impact angle and the erosion rate after blasting for 7200s at $V=100$ m/s and 145 m/s with ADI. At $V=145$ m/s and also at $V=100$ m/s, erosion rate reaches a maximum at $40^\circ\sim 60^\circ$ quite different from SS400. Compared with SS400 the erosion rate of ADI is, at $V=145$ m/s, 20%, and at $V=100$ m/s, it is 23%, very small values due to quite different phenomena. It is clear that impact angles does not have

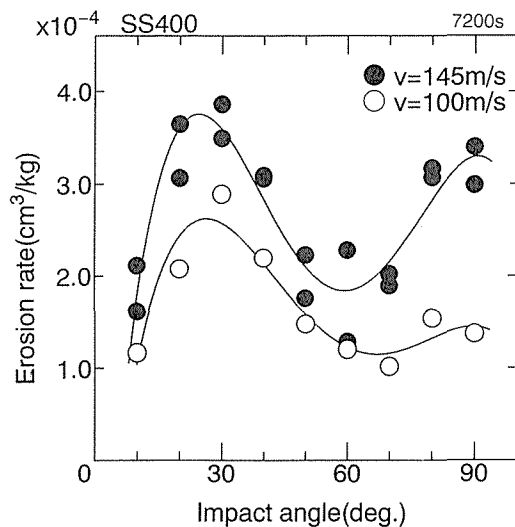


Figure 6 Erosion rate vs. impact angle, SS400

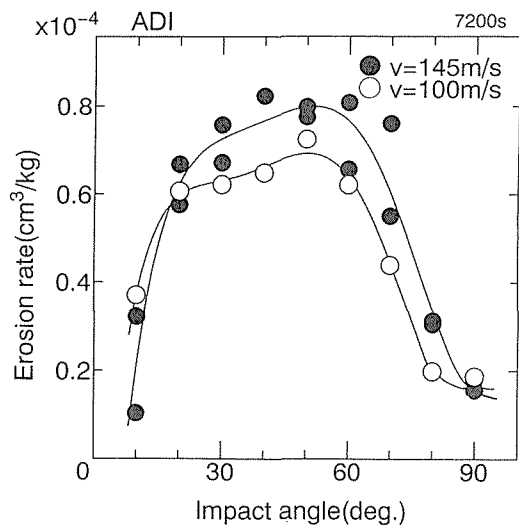


Figure 7 Erosion rate vs. impact angle, ADI

much influence on erosion rate and eliminate the effect of impact velocity.

4. Observation of the Eroded Surfaces

To evaluate the above results in relation to surface changes caused by erosion, the eroded surfaces were observed macroscopically.

Figure 8 shows the eroded surfaces of SS400 with $V=100$ m/s and 145 m/s after blasting for 7200s, at impact angles of 10° , 30° , 60° , and 90° . All the specimens show eroded area of the same size as the particle-impact area, irrespective of impact velocity. At $10^\circ\sim50^\circ$ impact angles, there are lamellar patterns across surface at toward the right angles to the blast direction. At $70^\circ\sim90^\circ$, there are no lamellar patterns. At 60° , there are lamellar patterns in the lower half, while upper half shows small dimples. From these observations, erosion characteristics, subjected to $10^\circ\sim50^\circ$ and $70^\circ\sim90^\circ$ impacts are different and the 60° impact angle is the border.

Figure 9 shows the eroded surfaces of ADI at $V=100$ m/s and 145 m/s blasting for 7200s. The impact angles are 10° , 30° , 60° and 90° . Like SS400, the impacted area is similar to the particle-impact area, irrespective of impact angle.

The appearance of the eroded surface of ADI is different from that of SS400, at 10° and 20° , it is quite smooth, at $30^\circ\sim50^\circ$, indistinct lamellar patterns can be seen and at $60^\circ\sim90^\circ$ the surface is covered with dimples. As shows in Figure 5, the erosion rates at $V=100$ m/s and

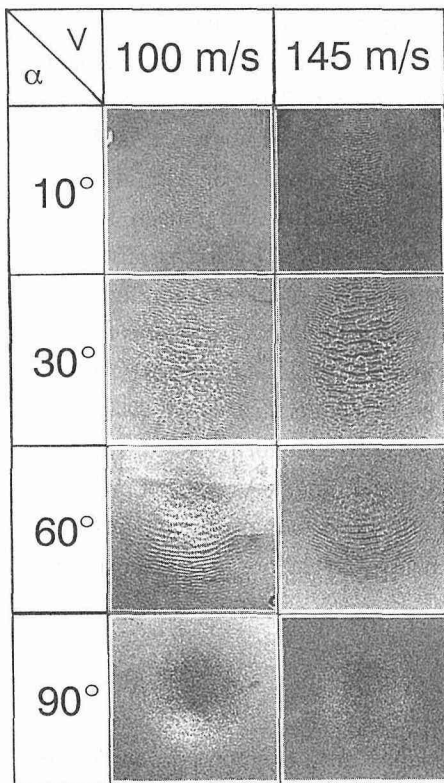


Figure 8 Macroscopic appearance of the eroded SS400 surface

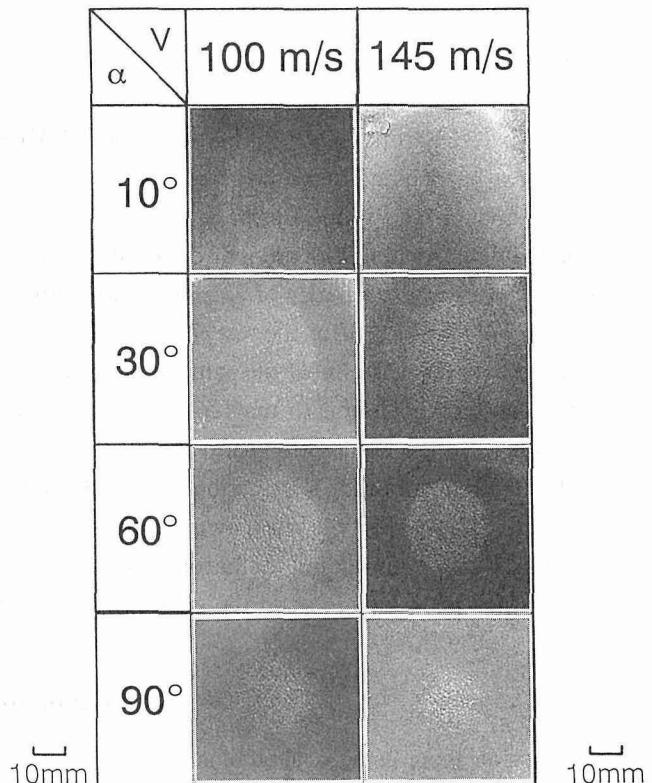


Figure 9 Macroscopic appearance of the eroded ADI surface

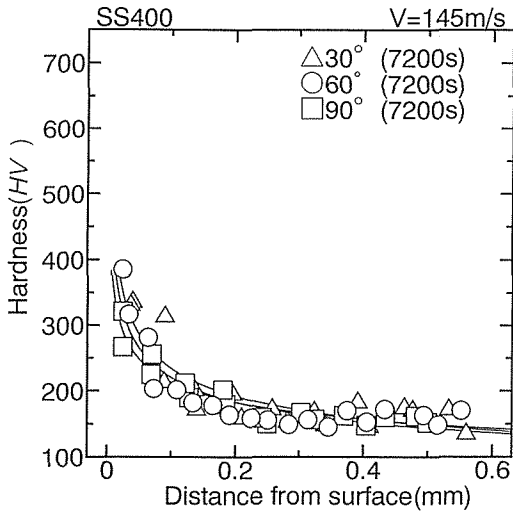


Figure 10 Hardness (HV) vs. distance from surface, SS400

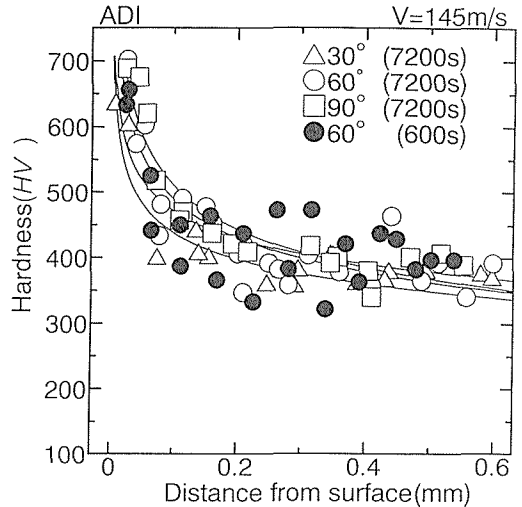


Figure 11 Hardness (HV) vs. distance from surface, ADI

145 m/s are not different, and the eroded surface of ADI does not show differences by of impact velocity. Therefore macroscopic observations are insufficient to elucidate the difference in the eroded surfaces.

To confirm the superior erosion resistance of ADI compared with SS400, the hardness near the surface was measured. Figure 10 and 11 show the hardness distribution of SS400 and ADI in the depth direction, for impact angles of 30°, 60°, 90° with 7200s of blasting. The initial Vickers hardness (HV) of SS400 is about HV150 but on the eroded surface, it is HV380, showing a hardening caused by the impacts. The initial hardness value of ADI is around HV350 and on the eroded surface it reaches HV750. To establish the reason for this remarkable hardening, the amount of retained austenite was measured by X-ray diffraction method. For impact angles of 30°, 60°, and 90°, there is about 40% of the matrix before the test, but only 3 to 5% after the test (7200s). The Micro-Vickers hardness test shows that the surface hardness was almost the same at 600s the value after at 7200s, and the transformation of the retained austenite to martensite is considered to be complete already at 600s. The results lead to the assumption that, the austenite on the surface transforms into martensite by the impacts, and that the erosion rate is slowed by the hardening. As erosion proceeds, the top martensite layer is worn away and the austenite in the under lying surface transforms into martensite maintaining the hardness to some depth below the surface. Further, impact velocity has little influence on the erosion rate of ADI.

5. Conclusion

Erosion tests using a shot blast machine was performed on austempered ductile iron (ADI) at various impact angles, and the results were compared with SS400. The erosion mechanism in the two materials, and the effect of impact velocity on it was discussed.

The results were as follows :

(1) Compared with SS400, the erosion rate of ADI, at $V=145$ m/s is 20% and, at $V=100$ m/s it is 23%.

(2) With ADI, the erosion rate reaches a maximum at $40^{\circ}\sim 60^{\circ}$ and $V=145$ m/s, quite different from the case of SS400. At $V=100$ m/s the erosion rate is similar, showing that the impact velocity has little influence on the erosion rate of ADI.

(3) The eroded surface of ADI is hardened by the particle impacts, and the austenite is transformed into martensite, reducing the erosion rate, and also eliminate the effect of impact velocity.

Acknowledgement

The authors wish to express their gratitude to Mr. Hideyuki Furui (Sumitomo 3M, L. t. d), Mr. Masato Goka (Hitachi Metals, L. t. d) and Takafumi Kamada (Hokkaido Univ. student) for their suggestions and advice in performing the experiments.

References

- 1) K. Shimizu, T. Noguchi, Trans. of AFS, 101 (1993), Paper No. 93-078
- 2) K. Shimizu, T. Noguchi et al, Proceedings of JSME, 920-78 (1992), 483
- 3) I. Finne, Wear, 3 (1960), 87-103
- 4) J. G. A. Bitter, Wear, 6 (1963), 5-21
- 5) J. G. A. Bitter, Wear, 6 (1963), 169-190
- 6) J. H. Neilson, A. Gilchrist, Wear, 11 (1968), 111
- 7) K. V. Pool, C. K. H. Dharan, I. Finne, Wear, 107 (1986), 1-12
- 8) T. H. Tsiang, ASTM STP 1003 (1989), 55-74
- 9) A. W. Ruff, L. K. Ives, Wear, 35 (1975), 195-199
- 10) S. Okazaki, K. Hasegawa, Trans. JSME, 56 (1990), 1668-1671
- 11) R. C. Tucker, ASM Metals Handbook, 11 (1986), 145-162
- 12) R. C. Tucker, ASM Metals Handbook, 11 (1986), 602-607